Ultrasonic attenuation in articular cartilage[a)]

David A. Senzig and Fred K. Forster
Department of Mechanical Engineering, University of Washington, Seattle, Washington 98195

John E. Olerud
Department of Medicine (Dermatology) and Department of Orthopaedics, University of Washington, Seattle, Washington 98195

(Received 24 January 1992; accepted for publication 14 April 1992)

Previous studies have utilized articular cartilage from joints as a model to investigate the influence of various constituents in a connective tissue matrix on ultrasonic properties. These studies have assumed a degree of homogeneity of articular cartilage taken from the same joint. However, tactile loads on articular cartilage vary significantly with location in a joint, and the effects of mechanical load on the connective tissue matrix and the resulting effects on ultrasonic properties are not known. This work reports the variations in acoustical properties of bovine articular cartilage from the stifle (knee) joint both among different joints and within each joint. A pulse-echo transmission technique was used to measure acoustic attenuation in the frequency range of 10 to 40 MHz. The attenuation coefficient was characterized by the integrated attenuation (mean value) over the frequency bandwidth considered. Integrated attenuation averaged over each joint varied among joints from 3.2 to 7.5 NP/cm (6.0 ± 2.0, mean $\pm$ s.d.). Additionally, a linear regression ($r = 0.59$) of all the data versus location along the patellar groove indicated that within joints integrated attenuation increased from proximal to distal locations by 6% to 60% (32 ± 25, mean $\pm$ s.d.). The variations observed among joints and along the patellar groove within a given joint suggest that studies utilizing articular cartilage to determine the role of connective tissue constituents on acoustic properties require control for joint and location. An additional outcome of this study was the observation that damage to the load-bearing surface of articular cartilage may be detectable ultrasonically through characteristics of the acoustic reflection from the articular surface.

PACS numbers: 43.80.Cs, 43.80.Ev, 43.80.Qf

INTRODUCTION

Collagen is the major structural constituent in connective tissue. It is present in the form of fibers that are constructed from fibrils, which in turn are composed of individual collagen molecules. The most common forms of molecular collagen are types I, II, and III. Most collagen exists as molecules in a helical arrangement of three monomers. The acoustic impedance of collagen fibers is significantly higher than that of most other soft tissue (Goss and O'Brien, 1979). The acoustic attenuation coefficient of collagen-rich tissue such as skin is also higher than other soft tissue with less collagen, such as liver (Daft *et al.*, 1989). Thus medical acoustic techniques of both the therapeutic or diagnostic variety are affected by the presence of collagen. Conversely, acoustic techniques that could quantify the amount of collagen or detect chemical or mechanical alterations in the state of connective tissue would be important for monitoring certain biological processes, such as wound healing (Forster *et al.*, 1990; Olerud *et al.*, 1990) and damage to cartilage surfaces, e.g., fibrillation (Freeman and Meachim, 1979).

The matrix of articular cartilage exists as a collagen framework primarily consisting of type II collagen. The structural, biochemical, and mechanical properties are reasonably well characterized, and enzymatic methods have been described to selectively extract from cartilage the glycosaminoglycans, proteoglycans, and other noncollagen proteins (Chun *et al.*, 1986). Additionally, the intramolecular crosslinks of the collagen framework can be selectively cleaved. Hence articular cartilage is an attractive and appropriate model for the acoustic study of the role of various connective tissue constituents on acoustic behavior. Results of Agemura *et al.* (1990) show that changes in collagen cross-linking result in significant changes in attenuation coefficient. These results assume homogeneity of articular cartilage taken from the same joint.

To ensure protocols developed to investigate acoustical properties of cartilage can be controlled for biological variations, it is important to determine joint-to-joint variations. In addition, a review of biomechanics indicates that loads vary significantly within a joint (Maquet, 1984). We speculated that the structure and acoustical properties of the cartilage may also be subject to variation within a joint. Thus, in this study the variation in acoustic attenuation coefficient both among different joints and within each joint was investigated.

[a)] Send requests for reprints to F. K. Forster.

 0001-4966/92/080676-06$00.80

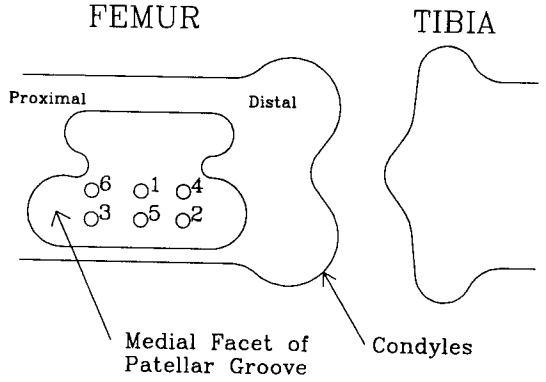

FIG. 1. Schematic of the patellar groove showing regions in the medial facet from which samples were taken. The entire medial facet was approximately 10×2 cm. Three locations along the patellar groove, proximal (regions 3 & 6), middle (regions 1 & 5), and distal (regions 4 & 2) are depicted from left to right. Spacing along the patellar groove (shown left to right) was 2–2.5 cm and between adjacent samples within each region (shown vertically) was approximately 1 cm.

I. METHODS

A. Specimen preparation

The articular cartilage specimens were obtained from the medical facet of the patellar groove of bovine stifle (knee) joints. The stifle joint is the articulation of the femur (thigh bone), the tibia (leg bone), and the patella (knee cap). The patellar groove is located on the distal femur (see Fig. 1) where it provides a channel to control the transverse motion of the patella. The cartilage that covers the medial facet of the patellar groove is approximately 10 cm long, 2 cm wide, and 1 mm thick. Morphological studies of adult articular cartilage show three different zones of preferred collagen fiber bundle orientation. At the articular surface a tangential zone representing approximately 20% of the thickness (approximately 200 μm) is present. Collagen fiber bundles in that zone are tightly packed and oriented approximately parallel to the surface. Beneath the tangential zone are the larger transitional and radial zones representing approximately 30% and 50% of the thickness (300 and 500 μm), respectively. In the radial zone the preferred collagen fiber bundles orientation is perpendicular to the articular surface. In the transitional zone, as the name implies, a transition in fiber bundle alignment occurs from parallel in the tangential zone to perpendicular in the radial zone. Hence, preferred fiber bundle orientation in the transitional zone is more random (Hukins *et al.*, 1984; Agemura *et al.*, 1990).

Five joints were obtained from a local meat packer (Weber Packing, Sumner, WA). The animals' ages were typical of slaughtered steers, i.e., from 1 to 2 years old. The stifle joints were removed and frozen to − 10 °C at the packer, then delivered to the University of Washington and processed immediately or stored at − 20 °C for up to 2 weeks before processing.

All cartilage specimens were removed from the medial facet of the patellar groove of each joint after it was thawed for 24 h at approximately 2 °C. Each sample was removed with a 4.0-mm-diam biopsy punch from a flap of cartilage separated from the subchondral bone with a scalpel. Immediately after removal each sample was placed in a separate plastic container, bathed in an embedding compound (Tek-Tissue OCT, Miles Co., Indiana), and then refrozen by dipping in a mixture of dry ice and ethyl alcohol and later stored in a freezer at − 70 °C until microtoming was performed. The time required to excise, embed, and refreeze each specimen was less than 30 min.

Preliminary studies indicated that the end (articular and chondral) surfaces required planing with a microtome to ensure that acoustic propagation through each sample was not significantly affected by surface roughness or convexity (Senzig, 1991). Microtoming was performed on the frozen samples. Approximately 25–60 μm was removed from each surface (in the tangential and radial zones, respectively) to provide two smooth, plane, and parellel surfaces.

A schematic of sample locations for each joint is shown in Fig. 1. Two samples were taken from each of three locations along the patellar groove. The proximal location corresponded to regions 3 and 6, the mid-location to regions 1 and 5, and the distal location to regions 2 and 4. The random numbering system was part of the protocol; the data reduction was performed blind without location information. The separation between proximal and distal locations ranged from 4 to 5 cm. The separation in the medial direction was approximately 1 cm.

B. Acoustical analysis

The acoustic measurements were performed with a single-transducer, pulse-echo system designed for high-resolution tissue characterization of skin. A Panametrics (Waltham, MA) pulse/receiver model 5600 and transducer model V375 were utilized. The transducer focal length was 1.9 cm, with an active element diameter of 0.64 cm. The − 6-dB beam width at the focus and the focal depth of field were measured to be 0.2 and 4.4 mm, respectively (Forster *et al.*, 1990). Further details are given elsewhere (Forster *et al.*, 1983; Senzig, 1991). Prior to the cartilage analysis, the system calibration was confirmed by comparing attenuation coefficient estimates for chloroform with published data. The comparison is shown in Fig. 2.

At the time of ultrasonic data acquisition each microtomed sample was thawed, and the embedding compound was removed using a buffered Tris-saline solution at room temperature. Each sample was then mounted with the chondral side (radial zone) contacting an optically smooth glass surface 0.24 cm thick. The 4-mm-diam specimen was held in place by a Lexan mounting plate having a 2.0-mm-diam acoustical access hole centered over the specimen. This dimension was small enough to ensure contact at the cartilage–glass interface, and yet large enough to allow examination of the sample without measurable interference with the acoustic beam. After mounting, the sample was lowered in a 20 °C degassed 0.15 M saline solution that served as a coupling medium between the transducer and the sample.

With the transducer focused on the glass mounting surface behind the specimen, five records of the specular reflection from the glass were digitized at five different lateral

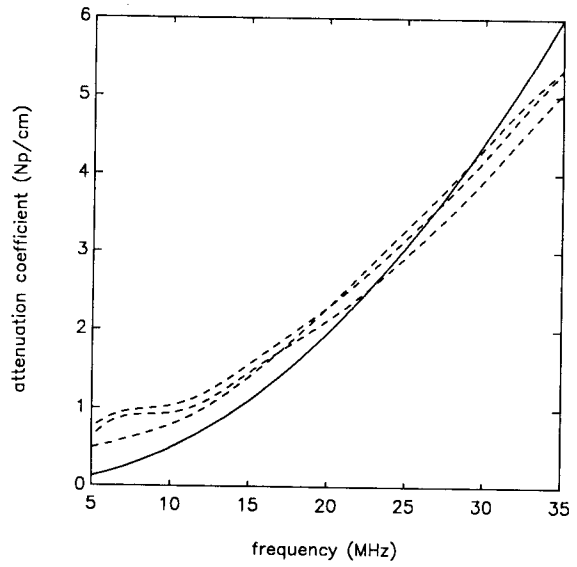

FIG. 2. Calibration data using measured values of the attenuation coefficient for chloroform ($CHCl_3$) are shown with dashed curves. Multiple calibration curves represent independent measurements. A best-fit curve by Huf-Desoyer *et al.* (1979) based on their data taken between 15 and 47 MHz is shown as a solid curve.

locations corresponding to the coordinates, (0.0,0.0) and ($\pm 0.3, \pm 0.3$) mm. Similarly, five time records were taken of the reference reflection from the glass before mounting of the specimen. The entire acoustical measurement process took approximately 15 min per sample after thawing.

The frequency-dependent attenuation coefficient $\alpha(f)$ was estimated for each sample as

$$\alpha(f) = \frac{1}{4t} \ln \frac{G_r(f)}{G_i(f)}, \tag{1}$$

where t is the specimen thickness, $G_r(f)$ is the average of the power spectral densities (PSD) of the five reflection time records, and $G_i(f)$ is the corresponding PSD with the specimen in place. This procedure corresponds to the *C*-scan averaging protocol of Forster *et al.* (1985). The PSD were based on 64-point time records sampled at 320 MHz. A 1024-point fast Fourier transform was used after eliminating signal offset, applying a Kaiser–Bessel data window, and adding trailing zeroes. The specimen thickness was determined from the acoustic speed in cartilage and the time delay observed between front and rear echoes. The acoustic wave speed through cartilage was taken as 1700 m/s (Agemura *et al.*, 1990).

For the purpose of investigating joint-to-joint and within joint variations in the attenuation coefficient, the integrated attenuation α_I was statistically analyzed. This variable was defined as the average over frequency of the attenuation coefficient

$$\alpha_I = \frac{1}{f_2 - f_1} \int_{f_1}^{f_2} \alpha(f) df. \tag{2}$$

The frequency range chosen in this study was 10 to 40 MHz, which represented the usable bandwidth of the pulse-echo system employed. While the details of the frequency dependence of $\alpha(f)$ are lost by the integration used to define α_I, the latter variable was considered a more robust estimate of attenuation than $\alpha(f)$ at a particular frequency. All statistical analyses were performed using a commercial statistical package (SYSTAT, Systat, Inc., Evanston, IL).

C. Error analysis

Three possible sources for error were identified with the transmission method used to estimate the plane reflector and comparing the reflected acoustic signal from the reflector with and without the specimen in place. Each error was expressed as a fractional error $E = (\alpha_{\text{true}} - \alpha_{\text{measured}})/\alpha_{\text{true}}$. A detailed description of each error is given by Senzig (1991). The error E_r was due to the acoustic impedance mismatch between saline and each cartilage specimen. It was expressed as

$$E_r = \ln T_I / 2\alpha t, \tag{3}$$

where T_I is the power transmission coefficient for saline/cartilage. A worst-case estimate of E_r was 3% based on $T_I = 0.996$, $t = 0.2$ mm, and $\alpha = 3$ Np/cm.

The fractional error E_c was due to curvature of the front surface of each cartilage specimen introduced by the force of the mounting jig at the outer edge of each specimen. The resulting error was based on the deviation Δt in local thickness t, and was expressed as

$$E_c = 1 - t/(t - \Delta t). \tag{4}$$

A worst-case estimate of E_c was 8% based on $t = 0.2$ mm and $\Delta t = 0.015$ mm.

The last error considered was denoted as E_g, and it was due to a fluid gap between the cartilage specimen and the plane reflector on which it was mounted. A gap smaller than the pulse duration can cause interference between incoming and reflected acoustic signals. However, since each specimen was held against the mounting reflector by the force of the jig, any fluid gap would be reduced to the order of the roughness of the microtomed surface, which was assumed to be approximately 5 μm. The resulting worst-case value of E_g was 1%.

The above error estimates do not include the effect of the uncertainly in wave speed which has a 90% confidence interval of 1620 to 1740 m/s (Agemura *et al.*, 1990). This uncertainty in wave speed and the resulting uncertainty in the thickness estimate t increased E_r and E_g, but the change was small relative to E_c.

When added together, the three measurement errors were estimated to be a maximum of 12% for a thin specimen with a low attenuation coefficient. These error estimates are consistent with the calibration data shown in Fig. 2 at middle frequencies where the spread of the data is approximately the same amount.

II. RESULTS

A box plot of the integrated attenuation α_I is shown in Fig. 3(a) for all joints. The data strongly suggested differences among joints. The mean for each joint varied from 3.2 Np/cm (joint 3) to 7.5 Np/cm (joint 1) (6.0 ± 2.0, mean $\pm$ s.d). A multiple-comparison test based on the Tu-

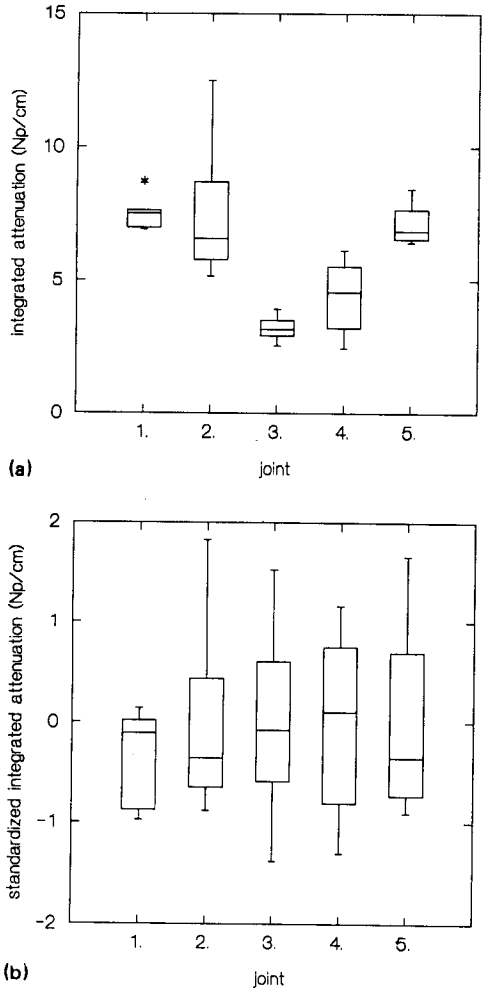

FIG. 3. (a) Raw integrated attenuation data. (b) Integrated attenuation standardized to a zero mean and unity standard deviation for each joint. The median is shown in each box, whose width marks the extent of half the data. The whiskers extend to data lying within another 1.5 box width. An asterisk marks a datum outside the whiskers.

key honestly significant difference (HSD) method indicated the means of joints three and four were different from joints one and two at the $P = 0.01$ level of significance. However, as Fig. 3(a) shows, the variance of the data differed among joints, making the HSD test not strictly valid, and a Bartlett test for the homogeneity of variances confirmed that the variances were different at the $P \leqslant 0.01$ level ($F = 4.6$, $DF = 4$).

Given the probable differences in the mean and variance of the attenuation coefficient among joints, and to investigate the effect of location within joints, α_I was standarized by joint by subtracting the mean for each joint and dividing by the standard deviation for each joint. The resulting dimensionless variable $\alpha_{I_{\text{std}}}$ had a mean of zero and a unit standard deviation for each joint. In addition, the one outlying datum shown in Fig. 3(a) was also removed. This procedure allowed further statistical analyses under the proper assumptions of homogeneous variance. The resulting variable $\alpha_{I_{\text{std}}}$ is shown in Fig. 3(b). An analysis of variance (ANOVA) was performed in which $\alpha_{I_{\text{std}}}$ was the dependent variable and joint and location along the patellar groove were

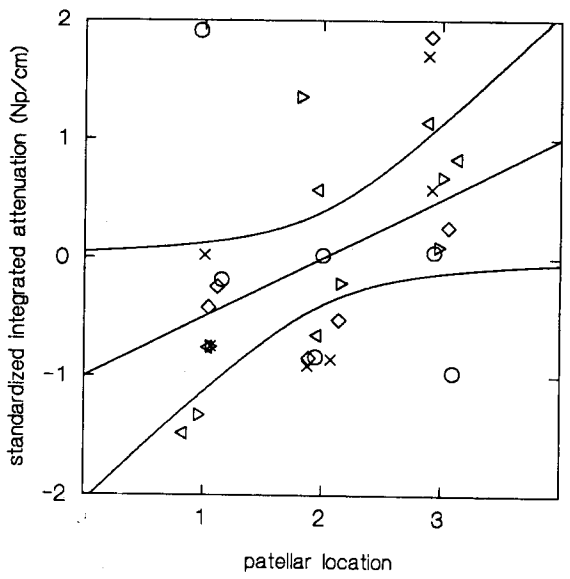

FIG. 4. Linear regression of standardized attenuation versus location along the patellar groove. Locations 1 = proximal (regions 3 & 6), 2 = middle (regions 1 & 5), and 3 = distal (regions 4 & 2). Slope = -1.338 and intercept = 0.627. Joint is indicated by the following notation: 1 = ○, 2 = ◇, 3 = ▷, 4 = ◁, and 5 = ×. The 95% confidence interval for additional data is also shown.

independent variables. The analysis was used to determine what portions of the total variance could be explained by joint and location effects. The results indicated that $\alpha_{I_{\text{std}}}$ was different with respect to location at a significance level of $P < 0.01$, and not significant with respect to joint ($P > 0.9$). The interaction between joint and location was also not significant ($P = 0.08$).

Based on the results above a linear regression of $\alpha_{I_{\text{std}}}$ versus patellar location was performed, and the result is shown in Fig. 4. A t test for the slope being zero was used to determine that the regression was statistically significant ($P = 0.001$). The Pearson correlation coefficient r was 0.59. Using the linear transformation relationship between standardized and nonstandardized attenuation, the predicted value of integrated attenuation for each joint versus location was determined. Based on this linear regression, the change in (nonstandardized) integrated attenuation from proximal to distal locations along the patellar groove of each joint ranged from 6% to 60% (32 ± 25, mean $\pm$ s.d.).

III. DISCUSSION

The results presented in Fig. 4 indicate that cartilage from the medial facet of the patellar groove appears to have an acoustic attenuation coefficient that increases from the proximal to the distal location. A change in attenuation coefficient along the patellar groove of the femur is consistent with current knowledge of the load distribution there. The forces exerted on the patellar groove are due to contact with the patella. In humans, the loads are highest on the patellar groove when the knee is bent and bearing weight, e.g., walking up a flight of stairs with one's weight carried by the bent knee. Under such conditions the patella is in its distal position along the patellar groove. The range of stresses along the

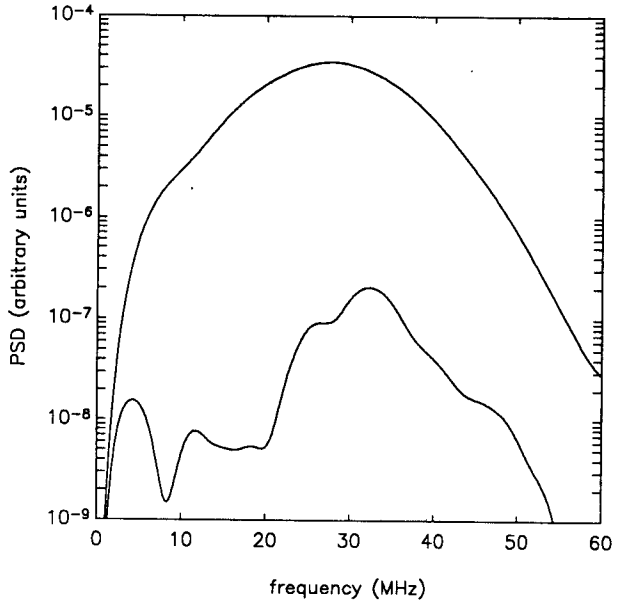

FIG. 5. Power spectral densities of the acoustic reflections from the articular surfaces of two nonmicrotomed cartilage specimens from the same joint.

patellar groove in the human knee during walking can vary by a factor of 6, from approximately 7 to 40 kPa (Townsend *et al.*, 1977; Maquet, 1984). While the reported stresses in human knees may be quantitatively different in the bovine stifle joint due to differences in the geometry, the basic components of the two joints are similar. Thus the stresses along the bovine patellar groove are also expected to increase in the distal direction.

The underlying reason for the attenuation coefficient to be higher in regions of higher stress is not known. However, the variation of load-dependent constituents in the cartilage matrix subjected to different loads may influence the acoustic properties. Macroscopically, load bearing in cartilage is accomplished through elastic resistance and creep. Both of these processes are related to the properties of proteoglycans (PG), which are hydrophilic structures attached to long chains of hyaluronic acid, which in turn are woven throughout the collagen fibers. PG and collagen are associated with the elastic behavior whereas PG and water are associated with creep (Mow *et al.*, 1990). The PG in the cartilage matrix predominantly influences the creep process through a frictional retardation of relative fiber motion (Schmidt *et al.*, 1990). This process has also been described by Weightman and Kempson (1979). Specific evidence of biochemical variations within a joint have been investigated by Droogendijk and Mow (1982). Their results indicate strong correlations between distance along the bovine patella (from the more highly loaded distal region to the more lightly loaded proximal region) and water content, uronic acid, permeability, elastic modulus, and thickness. Thus the observed variation in acoustic attenuation coefficient may be associated with structural variations in cartilage associated with load-bearing capability.

The statistically significant variation in the attenuation coefficient with joint and location within joint obtained in this study has major implications for basic studies of the relationships between cartilage structure and acoustic properties. Agemura *et al.* (1990) investigated the ultrasonic properties of cartilage at 100 MHz from two bovine stifle joint subjected to an enzyme extraction process to selectively remove macromolecules from the articular cartilage (Chun *et al.*, 1986). In that pilot study, four samples were taken from each patellar groove. For each joint one specimen served as the control and three received enzyme treatment. When standardized by joint with the method used in the current study, the attenuation coefficient for analogous samples (perpendicular orientation) ranged from -0.5 to 1.3 for joint A and from -0.82 to 1.45 for joint B. When compared to the present results shown in Fig. 4, these standardized values fall within the range of values observed in the current study over the length of the patellar groove. While differences existed in the methods used for the two studies, the enzyme treated samples did not yield results that exceeded the variations in the control joints of the present study.

Due to variations in acoustic properties among normal joints and along the patellar groove found in the current study, it would be optimal for each sample to serve as its own control if enzyme-treated cartilage samples are to be studied.

An additional finding of our work was that ultrasonics may be useful for diagnosing surface roughness, which may be an indicator of dysfunctional cartilage. In the current study, microtoming of the samples was necessary to eliminate detectable surface irregularities. The effect of such surface irregularities on the PSD of surface reflections from nonmicrotomed adjacent samples from the same joint are shown in Fig. 5. With the exception of having a nonmicrotomed articular surface, these two samples were prepared and analyzed as described in the methods section. In addition the sample thickness were approximately five times the pulse length. Even though the surfaces appeared visually identical, the PSD differ by two orders of magnitude and have a different frequency dependence. This indicates that surface defects (fibrillation) may be detectable. The lower spectrum shown in Fig. 5 cannot be completely explained by a simple model of surface irregularities smaller than the acoustic wavelength (Rayleigh, 1945). However, fibrillation may manifest itself as a more complicated frequency-dependent scattering process at the surface.

ACKNOWLEDGMENTS

This work was supported through NIH Grant No. AR39818. We are grateful to Larry Chun and Marcia Usui for their help with data collection and sample preparation.

Agemura, D. H., O'Brien, W. D., Olerud, J. E., Chun, L. E., and Eyre, D. E. (**1990**). "Ultrasonic Propagation Properties of Articular Cartilage at 100 MHz," J. Acoust. Soc. Am. **87**, 1786–1791.

Chun, L. E., Koob, T. J., and Eyre, D. R. (**1986**). "Sequential enzymic dissection of the proteoglycan complex from articular cartilage," Orthopaedic Trans. **10**(2), 257–258.

Daft, C. M. W., Briggs, G. A. D., and O'Brien, W. D. (**1989**). "Frequency dependence of tissue attenuation measured by acoustic microscopy," J. Acoust. Soc. Am. **85**, 2194–2201.

Droogendijk, L., and Mow, V. C. (**1982**). "Mapping of composition and biphasic material properties of cartilage over the patello-femoral groove," Proc. 28th Annual Orthop. Res. Soc., p. 151.

Forster, F. K., Olerud, J. E., and Gow, E. L. (**1983**). "Tissue Characterization of Skin utilizing High Ultrasonic Frequencies," in *Ultrasonics Symposium Proceedings*, edited by B. R. McAvoy (IEEE, New York), pp. 810–815.

Forster, F. K., Guttorp, P., and Gow, E. L. (**1985**). "Variance Reduction for Ultrasonic Attenuation Measurements from Backscatter in Biological Tissue," IEEE Trans. Sonics Ultrason. **SU-32**, 523–530.

Forster, F. K., Olerud, J. E., Riederer-Henderson, M. A., and Holmes, A. W. (**1990**). "Ultrasonic Assessment of Skin and Surgical Wounds Utilizing Backscatter Acoustic Techniques to Estimate Attenuation," Ultrasound Med. Biol. **16**, 43–53.

Freeman, M. A. R., and Meachim, G. (**1979**). "Aging and Degeneration," in *Adult Articular Cartilage*, edited by M. A. R. Freeman (Pitman Medical, London), Chap. 9, pp. 487–543.

Goss, S. A., and O"Brien, W. D. (**1979**). "Direct ultrasonic velocity measurements of mammalian collagen threads," J. Acoust. Soc. Am. **65**, 507–511.

Huf-Desoyer, V. G., Sedlacek, M., and Asenbaum, A. (**1979**). "Ultraschall-geschwindigkeit und Ultraschalldampfung in reinem Chloroform und in Chloroform-Arhanol-Mischungen," Acustica **45**, 327–332.

Hukins, D. W. L., Aspden, R. M., and Yarker, Y. E. (**1984**). "Fibre reinforment and mechanical stability in articular cartilage," Eng. Med. **13**, 153–156.

Maquet, P. G. (**1984**). *Biomechanics of the Knee* (Springer-Verlag, Berlin), 2nd ed., Chap. 4, p. 70.

Mow, V. C., Setton, L. A., Ratcliffe, A., Buckwalter, J. A., and Howell, D. S. (**1990**). 'Structure-function relationships of articular cartilage and the effects of joint instability and trauma on cartilage function," in *Cartilage Changes in Osteoarthritis*, edited by D. K. Brandt (Univ. of Indiana, Indianapolis), pp. 22–42.

Olerud, J. E., O'Brien, W. D., and Riederer-Henderson, M. A. (**1990**). "Correlation of Tissue Constituents with the Acoustic Properties of Skin and Wound," Ultrasound Med. Biol. **16**, 55–64.

Rayleigh, J. W. S. (**1945**). *Theory of Sound* (Dover, New York), Vol. 2, pp. 89–96.

Schmidt, M. B., Mow, V. C., Chun, L. E., and Eyre, D. R. (**1990**). "Effects of proteoglycan extraction on the tensile behavior of articular cartilage," J. Orthop. Res. **8**, 353–363.

Senzig, D. A. (**1991**). "Ultrasonic Attenuation in Bovine Articular Cartilage," M.S. thesis in Mech. Eng., Univ. of Washington.

Townsend, P. R., Rose, R. M., Radin, E. L., and Paux, P. (**1977**). "The biomechanics of the human patella and its implication for Chondromalacia," J. Biomech. **10**, 403–407.

Weightman, B., and Kempson, G. E. (**1979**). "Load carriage," in *Adult Articular Cartilage*, edited by M. A. R. Freeman (Pitman Medical, London), Chap. 5, pp. 291–331.